Journal of Chromatography A, 1224 (2012) 11–18

Contents lists available at SciVerse ScienceDirect

Journal of Chromatography A

journal homepage: www.elsevier.com/locate/chroma

Pseudomorphic synthesis of monodisperse magnetic mesoporous silica microspheres for selective enrichment of endogenous peptides

Gang-Tian Zhu [a], Xiao-Shui Li [a], Qiang Gao [a,b], Ning-Wei Zhao [c], Bi-Feng Yuan [a], Yu-Qi Feng [a,*]

[a] Key Laboratory of Analytical Chemistry for Biology and Medicine (Ministry of Education), Department of Chemistry, Wuhan University, Wuhan 430072, China
[b] Faculty of Material Science & Chemistry Engineering, China University of Geosciences, Wuhan 430074, China
[c] Life Science & Clinical Medicine Dept., Shimadzu (China) Co., Ltd, Shanghai, China

ARTICLE INFO

Article history:
Received 16 October 2011
Received in revised form 6 December 2011
Accepted 13 December 2011
Available online 20 December 2011

Keywords:
Magnetic mesoporous silica
Pseudomorphic transformation
Enrichment of endogenous peptides
MALDI-TOF mass spectrometry

ABSTRACT

In this work, we describe a novel synthetic strategy of magnetic mesoporous silica spheres (Fe_3O_4@$mSiO_2$) for the selective enrichment of endogenous peptides. Fe_3O_4 particles were coated with silica shell by a sol–gel method, followed by pseudomorphic synthesis to transform nonporous silica shell into ordered mesoporous silica shell. The core/shell structure and mesostructure were individually fabricated in two steps, which can be expedient to independently optimize the properties of monodispersion, magnetization and mesostructure. Actually, it was confirmed that the produced Fe_3O_4@$mSiO_2$ particles possess good monodispersion, high magnetization, superparamagnetism, uniform accessible mesopores, and large surface area and pore volume. With these good properties, Fe_3O_4@$mSiO_2$ spheres were applied to the rapid enrichment of peptides. Based on the size-exclusion mechanism and hydrophobic interaction with siloxane bridge group mainly on the surface of inside pores, Fe_3O_4@$mSiO_2$ can selectively capture peptides and exclude high-MW proteins and salts. Furthermore, peptides in human plasma were successfully enriched by Fe_3O_4@$mSiO_2$.

1. Introduction

The study of endogenous peptides in biological samples performs a crucial role in peptidomics [1–3], because of the new concept for the endogenous peptides from "biological trash" to "rich untapped source of disease-specific diagnostic information" [4]. However, the complexity and high dynamic range of biological samples make the characterization of endogenous peptides be a challenging task. Therefore, it is important to extract and enrich these peptides by appropriate methods prior to systematic peptidomics analysis. Ordered mesoporous silica materials, which possess easily modified surface, ordered pores, large surface area and pore volume, are widely applied in catalysis, adsorption, sensor, drug delivery, etc. [5–9]. Currently, highly ordered mesoporous silica materials have been successfully applied for separation of peptides from complex biological samples based on the combination of size-exclusion mechanism and the hydrophobic interaction with siloxane bridge group mainly on the surface of inside pores [10–13,3]. Meanwhile, magnetic particles have aroused great interest because of the property of low toxicity, biocompatibility and magnetic separability [14–18]. Undoubtedly, the combination of mesoporous morphology and magnetic property can generate a new class of separation materials with great application potential [19–24]. In the previous works, magnetic mesoporous silica particles have been applied to the enrichment of endogenous peptides, making the isolation of trapped peptides from sample solution convenient and fast [25–28].

Up to now, mainly two synthetic strategies have been applied to the preparation of magnetic mesoporous silica spheres. One strategy is to directly introduce magnetic particles into prepared mesoporous silica, which may result in pores clogging, small pore volume, pore structure distortion and poor magnetic response due to the difficulty in increasing Fe_3O_4 mass fraction [22,29–31]. An alternative strategy is to coat magnetic core with surfactant-templated mesophase silica shell in one step via a sol–gel process, and then the surfactant is removed to form mesoporous silica shell [24,32–36]. However, this approach needs to simultaneously optimize the fabrication of desired surfactant-templated mesophase and the formation of monodisperse spheres, which makes the morphological control difficult. In Lu group's work, magnetic mesoporous organosilica spheres were fabricated by coating Fe_3O_4 nanocrystals with mesoporous oganosilica [24]. The saturation magnetization value of the final product increased with the increased amount of Fe_3O_4, whereas the morphology became irregular. More recently, nonporous silica-coated Fe_3O_4 core (Fe_3O_4@$nSiO_2$) was further coated with surfactant-templated mesophase silica to fabricate Fe_3O_4@$nSiO_2$@$mSiO_2$ [35,36]. The obtained material had high magnetization and ordered

* Corresponding author. Tel.: +86 27 68755595; fax: +86 27 68755595.
E-mail address: yqfeng@whu.edu.cn (Y.-Q. Feng).

0021-9673/$ – see front matter © 2011 Elsevier B.V. All rights reserved.
doi:10.1016/j.chroma.2011.12.045

mesostructure, but the monodispersion was not satisfactory, which may limit its applications. Therefore, it is desirable and significant to prepare magnetic mesoporous silica with good monodispersion, high magnetization value and ordered mesostructure.

Pseudomorphism is well known in mineralogy, as it allows the preparation of a mineral with a desired morphology that is not related to its crystalline form [37]. Recently, the concept of pseudomorphic transformation (P-T) has been applied to various particle sizes of amorphous silica to produce ordered mesoporous silica. Pseudomorphic synthesis can independently optimize the processes of particle shaping and mesophase self-assembly [38,39]. Inspired by the advantages of the P-T method, herein, we report a novel synthetic strategy for the preparation of monodisperse Fe_3O_4@mSiO_2 microspheres. Fe_3O_4 particles were coated with silica shell by a sol–gel method, followed by pseudomorphic synthesis to transform nonporous silica shell into ordered mesoporous silica shell. Different from the previous methods, the fabrications of core/shell structure and mesostructure were controlled by two individual steps, which would be expedient to independently optimize the properties of monodispersion, magnetization and mesostructure. Actually, the obtained Fe_3O_4@mSiO_2 possesses good monodispersion, high magnetization, superparamagnetism, uniform accessible mesopores, and large surface area and pore volume, which makes it remarkable for the rapid and selective enrichment of peptides from complex biological samples.

2. Experimental

2.1. Reagents and materials

Ferric trichloride hexahydrate ($FeCl_3{\cdot}6H_2O$), sodium acetate (NaAc), ethylene glycol (EG), polyethylene glycol (PEG), cetyltrimethylammonium bromide (CTAB), ethanol (EtOH), ammonia hydrate ($NH_3{\cdot}H_2O$), sodium hydroxide (NaOH), ammonium nitrate (NH_4NO_3), sodium chloride (NaCl) and other chemicals were supplied by Shanghai General Chemical Reagent Factory (Shanghai, China). Tetraethyl orthosilicate (TEOS) was obtained from the Chemical Plant of Wuhan University (Wuhan, China). HPLC grade acetonitrile (ACN) was obtained from Fisher Scientific (Pittsburgh, PA, USA). α-Cyano-4-hydroxycinnamic acid (CHCA), trifluoroacetic acid (TFA), Angiotensin II, lysozyme, myoglobin, horseradish peroxidase (HRP) and bovine serum albumin (BSA) were purchased from Sigma–Aldrich (St. Louis, MO, USA). Sequencing grade trypsin was obtained from Promega (Madison, WI, USA). Human plasma sample was obtained from the Wuhan Zhongnan Hospital according to their standard clinical procedures and stored at −70 °C until further use. Purified water was obtained with a Millipore Milli-Q apparatus (Bedford, MA, USA).

2.2. Preparation of magnetite microspheres

The magnetite microspheres were prepared through solvothermal reaction [40] described as following: $FeCl_3{\cdot}6H_2O$ (5.40 g) was dissolved in ethylene glycol (160 mL) under magnetic stirring for 0.5 h. Then NaAc (14.40 g) and polyethylene glycol (4.0 g) were added to the solution. After stirring for another 0.5 h, the resultant solution was transferred into a Teflon lined stainless-steel autoclave with capacity of 200 mL. The autoclave was sealed and heated at 200 °C for 24 h, and then cooled to room temperature. The magnetic microspheres were collected with the help of magnet, followed by washing with recycle of ethanol and deionized water for 4 times, then the product was dried in vacuum at 60 °C for 8 h.

Table 1
Surface areas and pore volumes of Fe_3O_4@mSiO_2-*x* particles prepared at various molar ratio of NaOH/SiO_2.

Sample	NaOH/SiO_2	Surface area (m^2/g)	Pore volume (cm^3/g)
Fe_3O_4@mSiO_2-1	0.10	213	0.34
Fe_3O_4@mSiO_2-2	0.15	430	0.57
Fe_3O_4@mSiO_2-3	0.20	450	0.61
Fe_3O_4@mSiO_2-4	0.25	498	0.71
Fe_3O_4@mSiO_2-5	0.30	578	0.79

2.3. Preparation of Fe_3O_4@nSiO_2

Magnetic microspheres coated with nonporous silica (Fe_3O_4@mSiO_2) were synthesized through Stöber method with minor modification [41,42]. Briefly, Fe_3O_4 (120 mg) was homogeneously dispersed in a mixture of ethanol (467 mL), deionized water (139 mL) and $NH_3{\cdot}H_2O$ solution (15 mL). Then this dispersion was homogenized by vigorously stirring for 30 min. Finally, under continuous mechanical stirring, TEOS (6.0 mL) was slowly added to this dispersion, and after stirring for 8 h at room temperature, silica was formed on the surface of Fe_3O_4 through hydrolysis and condensation of TEOS. The Fe_3O_4@nSiO_2 particles were washed by ethanol and deionized water for several times, and then dried in vacuum at 60 °C for 8 h. The mass fraction of silica in Fe_3O_4@nSiO_2 can be estimated via the mass difference between Fe_3O_4 and Fe_3O_4@nSiO_2.

2.4. Preparation of Fe_3O_4@mSiO_2

Fe_3O_4@nSiO_2 spheres were converted into Fe_3O_4@mSiO_2 particles according to pseudomorphic transformations by hydrothermal reaction, using silica shell of Fe_3O_4@nSiO_2 particles as the source of silica. The molar ratio of all components was 1 SiO_2:0.1–0.3 NaOH:0.1 CTAB:80 H_2O, while the weight of SiO_2 was calculated by taking off the mass of Fe_3O_4 from that of Fe_3O_4@nSiO_2. The influence of the molar ratio of NaOH/SiO_2 was investigated (Table 1). Typically, when the molar ratio of all components was 1 SiO_2:0.2 NaOH:0.1 CTAB:80 H_2O, Fe_3O_4@nSiO_2 spheres (0.400 g of SiO_2) were added to a mixture of CTAB (0.243 g), water (9.6 mL), and NaOH (0.054 g) and stirred at room temperature for 30 min. The hydrothermal reaction was carried out in a Teflon-lined autoclave at 130 °C for 24 h. The products were recovered with the help of magnet and purified by multiple cycles of washing with ethanol and deionized water. Finally, the purified microspheres were redispersed in 50 mL of NH_4NO_3 ethanol solution (0.2 wt.%) and heated at 60 °C for 0.5 h to remove the template CTAB. This step was repeated for six times and CTAB was successfully removed. After the microspheres were washed with deionized water for 2 times, Fe_3O_4@mSiO_2 microspheres were finally obtained.

2.5. Characterization

Scanning electron microscopy images were taken using JSM-6700F field emission scanning electron microscope (FESEM, JEOL, Japan). Transmission electron microscopy images were obtained from JEM-2010 (HT) transmission electron microscope (TEM, JEOL, Japan). The powder X-ray diffraction (XRD) measurements were recorded on a D/MAX-RB X-ray powder diffractometer (RIGAKU, Japan) using Cu K_α radiation (λ = 1.5406 Å) with scattering angles (2θ) of 0.5–5°. Magnetic characterization was carried out using a Physical Property Measurement System (PPMS, Quantum design) with fields up to 20,000 Oe and at a temperature of 300 K. Nitrogen sorption measurement was performed at 77 K using a JW-BK surface area and pore size analyzer (JWGB Sci. & Tech., Beijing, China). The composites were activated by evacuating in vacuum

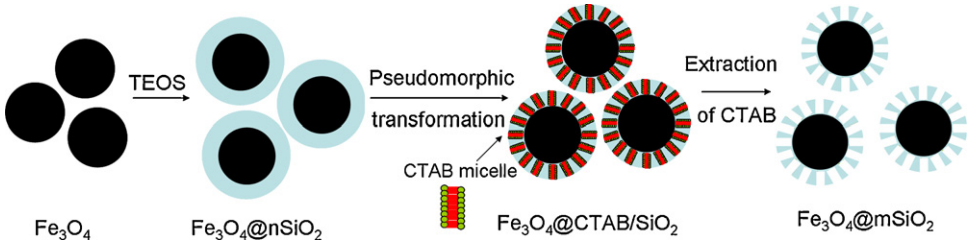

Fig. 1. Schematic diagram for the preparation of monodisperse Fe_3O_4@mSiO$_2$ microspheres.

and heating to 423 K for 6 h to remove any physically adsorbed substances before analysis. The specific surface area value was calculated according to the BET (Brunauer–Emmett–Teller) equation at P/P_0 between 0.05 and 0.3. The pore parameters (pore volume and pore diameter) were evaluated from the desorption branch of isotherm based on BJH (Barrett–Joyner–Halenda) model.

2.6. Preparation of peptides

BSA (1 mg) was dissolved in 100 μL of denaturing buffer solution (8 M urea in 100 mM Tris–HCl pH 8.5). The obtained protein solution was mixed with 5 μL of 100 mM tri(2-chloroethyl)phosphate (TCEP) and incubated for 20 min at room temperature to reduce protein disulfide bonding. Iodoacetamide (3 μL of 500 mM stock) was added, and the obtained solution was incubated for an additional 30 min at room temperature in the dark. The reduced and alkylated protein mixture was diluted with 100 mM Tris–HCl pH 8.5. Subsequently, 9 μL of 100 mM $CaCl_2$ was added, and the digestion mixture (~50 μL in volume) was digested by incubating overnight at 37 °C with trypsin at an enzyme to substrate ratio of 1:50 (w/w).

2.7. Enrichment of peptides from standard peptide solution

Aqueous solution of Angiotensin II (400 μL, 5 fmol/μL) was mixed with suspension of Fe_3O_4@mSiO$_2$-3 microspheres (2 μL, 5 mg/mL, in water), and shaken at room temperature for 3 min. At the same time, Fe_3O_4@nSiO$_2$ particles (2 μL, 5 mg/mL, in water) were used for comparison. After decanting the supernatant with the help of magnet, the residue was rinsed with water for three times as following: the residue was mixed with 200 μL water and shaken, and then the supernatant was decanted. The peptides trapped on the silica surface were eluted with 5 μL 50% ACN aqueous solution containing 0.1% TFA. Finally, original solution and eluates were directly applied onto the stainless steel target probe for MALDI-TOF MS analysis.

2.8. Investigation of the size-exclusion effect of Fe_3O_4@mSiO$_2$-3 microspheres

BSA digest (aqueous solution, 10 fmol/μL, 200 μL) or protein (aqueous solution, 0.5 pmol/μL, 200 μL) was mixed with suspension of Fe_3O_4@mSiO$_2$-3 microspheres (5 μL, 5 mg/mL, in water), and shaken at room temperature for 3 min. After decanting the supernatant, the residue was successively washed with 200 μL H_2O three times and the trapped peptides were eluted with 10 μL 0.1% TFA-50% ACN subsequently. The eluate was separated from particles with the help of magnet. Finally, original solutions, supernatants and eluates, were directly applied onto the stainless steel target probe for MALDI-TOF MS analysis.

2.9. Study of the desalting efficiency of Fe_3O_4@mSiO$_2$-3

BSA digest (10 fmol/μL, 200 μL) containing 1 M NaCl or 1 M urea was mixed with suspension of Fe_3O_4@mSiO$_2$-3 microspheres (5 μL, 5 mg/mL, in water), and shaken at room temperature for 3 min. After decanting the supernatant, the residue was washed with H_2O three times and eluted with 10 μL 0.1% TFA-50% ACN. For comparison, commercial Zip-Tip C18 pipette tips were used in the same condition according to the standard procedure (see Supporting Information). Finally, the eluted solutions were directly applied onto the stainless steel target probe for MALDI-TOF MS analysis.

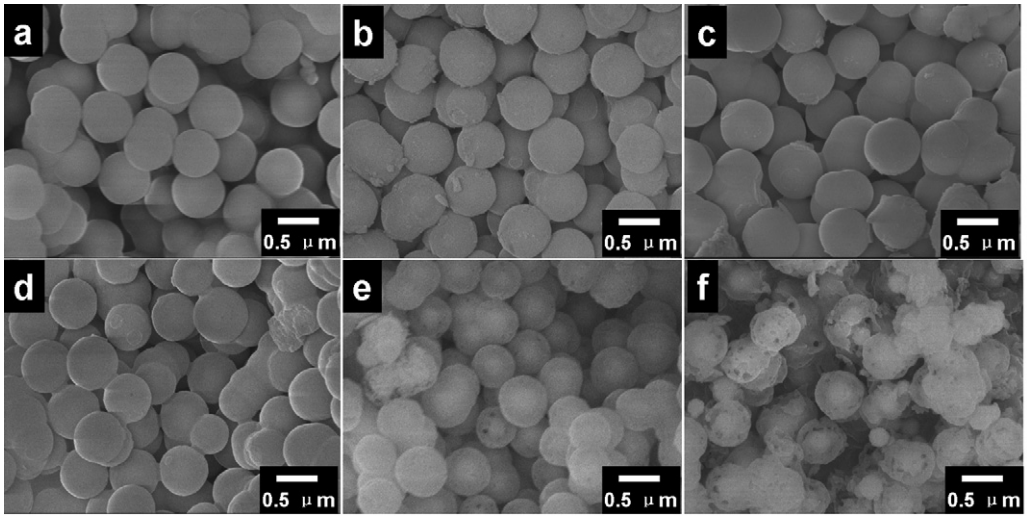

Fig. 2. SEM images of Fe_3O_4@nSiO$_2$ (a), Fe_3O_4@mSiO$_2$-1 (b), Fe_3O_4@mSiO$_2$-2 (c), Fe_3O_4@mSiO$_2$-3 (d), Fe_3O_4@mSiO$_2$-4 (e) and Fe_3O_4@mSiO$_2$-5 (f).

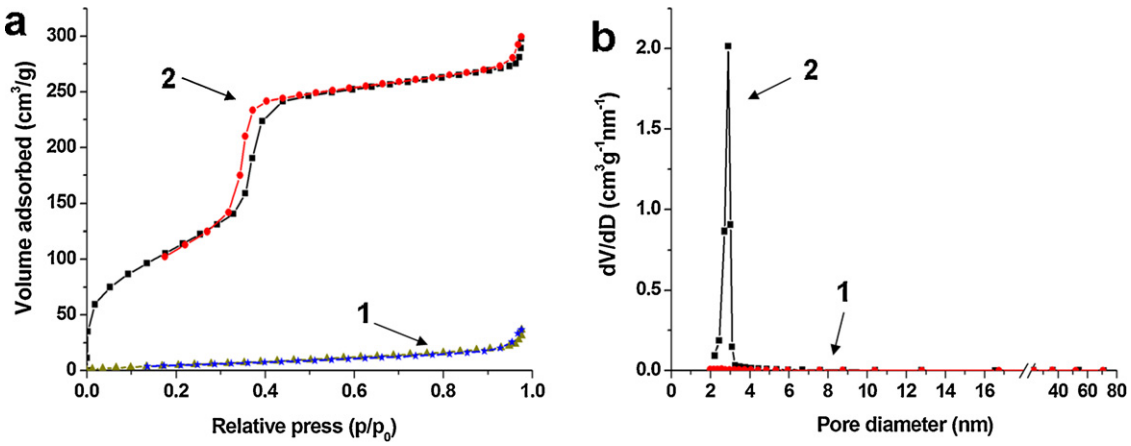

Fig. 3. N_2 adsorption–desorption isotherms of Fe_3O_4@nSiO_2 (1, a) and Fe_3O_4@mSiO_2-3 (2, a), and pore size distribution of Fe_3O_4@nSiO_2 (1, b) Fe_3O_4@mSiO_2-3 (2, b).

2.10. Rapid enrichment of peptides in human plasma

Human plasma (50 μL) was diluted with 350 μL H_2O, and then 10 μL suspension of Fe_3O_4@mSiO_2-3 microspheres (5 mg/mL) was added. Then, the supernatant was decanted and the microspheres were collected and rinsed. After that, the adsorbed peptides were eluted with 10 μL 0.1% TFA-50% ACN. Finally, the eluted solution was directly applied onto the stainless steel target probe for MALDI-TOF MS analysis.

2.11. MALDI MS analysis

Sample solutions (peptides or protein) were deposited on the stainless steel target probe using the dried droplet method. Sample solution (1 μL) was applied onto the target, and then 1 μL of CHCA matrix solution (2 mg/mL, 0.1% TFA in 50% ACN/H_2O solution) was introduced. All MALDI-TOF MS spectra were collected with an Axima TOF^2 mass spectrometry (Shimadzu, Kyoto, Japan). The instrument was equipped with a 337 nm nitrogen laser with a 3 ns pulse width. All the mass spectra were obtained in positive ion mode with an accelerating voltage of 20 kV. Typically, 200 laser shots were averaged to generate each spectrum. Analysis of peptides and proteins was performed in the reflector and linear TOF detection modes, respectively.

3. Results and discussion

3.1. Synthesis and characterization of Fe_3O_4@mSiO_2

The synthesis procedure is shown in Fig. 1. At first, magnetite particles were produced by a solvothermal reduction method. Afterwards, nonporous silica shell was coated on Fe_3O_4 microspheres according to a sol–gel method. Then, the P-T procedure was directly adapted from the synthesis of MCM-41 [38], by using the shell of Fe_3O_4@nSiO_2 particles as the source of silica. In the P-T procedure, silica was dissolved by the alkaline solution, and the resulting silicate species interacted with the surfactant CTAB and condensed into ordered mesophase [37]. Therefore, Fe_3O_4@nSiO_2 was transformed into mesophase coated magnetic microspheres (Fe_3O_4@CTAB/SiO_2). Finally, the template CTAB was fast removed by ammonium nitrate ethanol solution, and Fe_3O_4@mSiO_2 spheres were obtained.

Fig. 2a shows that as-prepared Fe_3O_4@nSiO_2 spheres are discrete and uniform in size and shape. The average size of the spheres is around 500 nm. In the P-T procedure, the effect of the molar ratio of NaOH/SiO_2 in a range of 0.1–0.3 on the morphology of the final product (Fe_3O_4@mSiO_2-*x*, *x* = 1–5) was investigated (Table 1). As shown in the SEM images (Fig. 2b–f), when the molar ratio of NaOH/SiO_2 in the pseudomophic synthesis is between 0.1 and 0.25, the produced Fe_3O_4@mSiO_2 spheres retain the same spherical morphology and granulometric distribution as the parent Fe_3O_4@nSiO_2 spheres. Notably, the monodispersion of Fe_3O_4@mSiO_2 spheres is the same as that of Fe_3O_4@nSiO_2. When the ratio of NaOH/SiO_2 is raised to 0.3, the structure of silica shell is destroyed. So the recommended value of NaOH/SiO_2 in the pseudomophic synthesis is inferior to 0.25. Typically, we chose Fe_3O_4@mSiO_2-3, which was prepared under the condition that the molar ratio of NaOH/SiO_2 was 0.2, for future characterizations and tests. According to the TEM image (Fig. S1a, SI), the core/shell structure of Fe_3O_4@nSiO_2 spheres can be clearly distinguished. The average diameter of magnetic core is about 300 nm, and the thickness of the silica shell is around 100 nm. As presented in Fig. S1b (SI), the macroscopic morphology of core/shell structure did not change after the P-T reaction. Additionally, Fig. S1c (SI) further confirms that mesoporous channels align in an orderly fashion in the silica shell and arrange perpendicularly to the surface, which makes the pores accessible for absorption and separation. Therefore, the P-T transformation did not change the macroscopic morphology of the parent silica source Fe_3O_4@nSiO_2, because the equilibrium of dissolution/condensation of silica can be controlled by the reaction conditions. However, when the amount of NaOH was excessive, the equilibrium of dissolution/condensation of silica would be destructed and the silica shell would be damaged. Briefly, under proper experiment conditions, the macroscopic morphology of final product including particle size and core/shell structure were determined by the synthesis step of Fe_3O_4@nSiO_2, while the microscopic morphology such as pore structure depended on the step of P-T reaction.

The N_2 sorption–desorption isotherms of Fe_3O_4@nSiO_2 and Fe_3O_4@mSiO_2-*x* were measured. The Brumauer–Emmett–Teller (BET) surface area of Fe_3O_4@nSiO_2 was found to be 25.0 m^2/g and the pore structure was nonporous (Fig. 3). After P-T reaction, the surface area increases obviously. As listed in Table 1, the surface area and pore volume of Fe_3O_4@mSiO_2-*x* increase with the increased molar ratio of NaOH/SiO_2. As mentioned above, the function of the alkaline solution is to dissolve silica, so increasing the amount of NaOH can promote more proportion of the silica shell dissolved and then converted into surfactant-silica mesophase, which may result in larger surface area and pore volume. Moreover, the nonporous pore structure was converted into ordered mesostructure after P-T reaction. Typically, N_2 sorption–desorption isotherms reveal IV-type curve for as-prepared Fe_3O_4@mSiO_2-3 spheres (Fig. 3a), indicating the presence of mesostructure [43]. The narrow and sharp pore size distribution curve (Fig. 3b), which

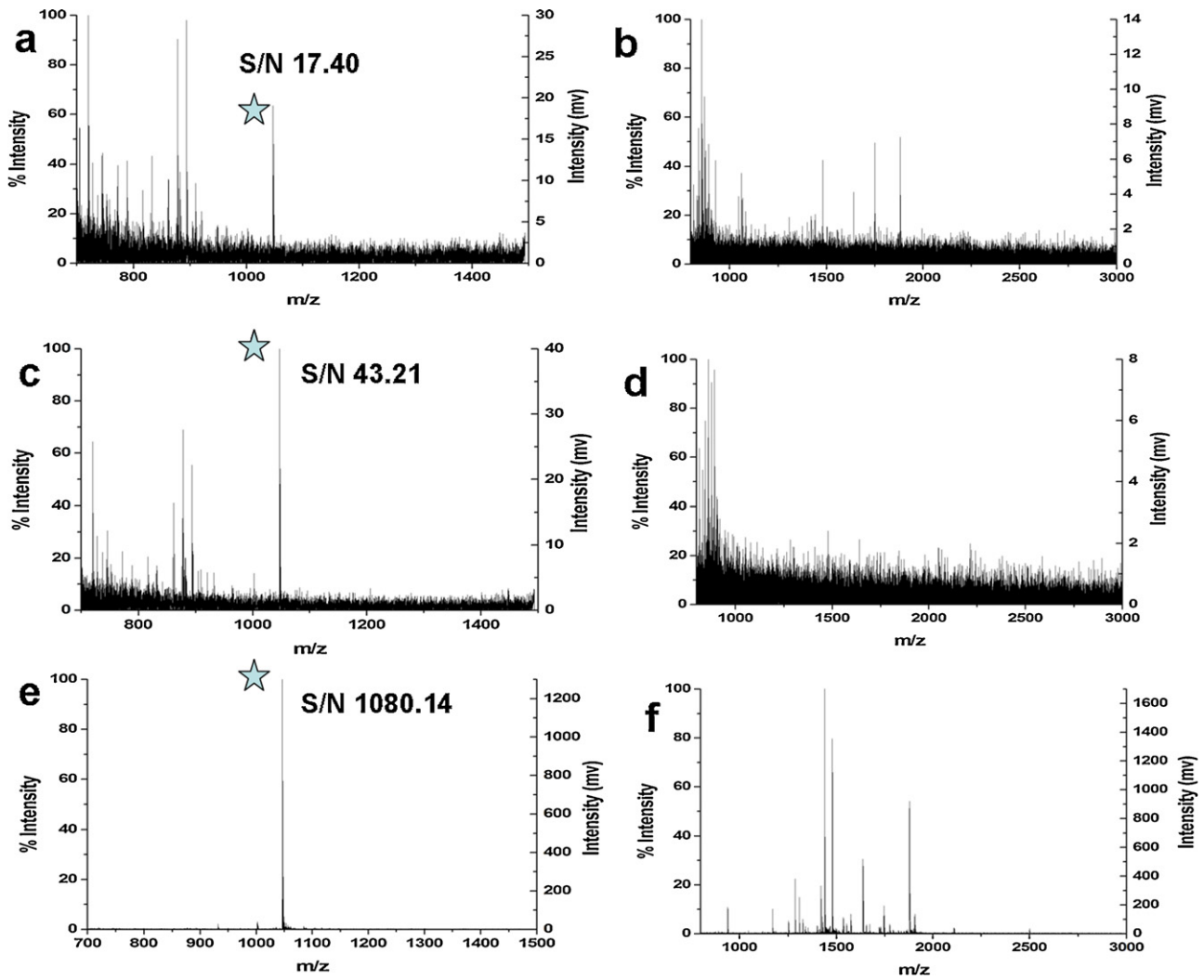

Fig. 4. MALDI-TOF mass spectra of 5 nM Angiotensin II without any treatment (a), enriched by Fe_3O_4@nSiO_2 (c) and Fe_3O_4@mSiO_2-3 microspheres (e), mass spectra of 10 nM BSA digest without any treatment (b), supernate (d) and eluate (f) after enrichment with Fe_3O_4@mSiO_2-3 particles. Asterisks mark the peaks of the standard peptide.

centers at the mean value of 2.9 nm, suggests that the mesopores have very uniform sizes. The ordered mesostructure of Fe_3O_4@mSiO_2-3 microspheres was further confirmed by low-angle XRD pattern (Fig. S2, SI). One high-intensity diffraction peak of (1 0 0) and two additional diffraction peaks of (1 1 0), (2 0 0) are observed, which can be assigned to a two-dimensional hexagonal mesostructure (space group p6mm).

The field-dependent magnetization curves measured at 300 K indicate that the saturation magnetization values of Fe_3O_4, Fe_3O_4@nSiO_2 and Fe_3O_4@mSiO_2-3 particles are 78.6, 37.4 and 47.1 emu/g (Fig. S3, SI), respectively. When the Fe_3O_4 particles were coated with silica to form Fe_3O_4@nSiO_2, the magnetization value reduced. Meanwhile, after P-T procedure, Fe_3O_4@nSiO_2 spheres were converted into Fe_3O_4@mSiO_2-3, which resulted in the increase of magnetization value. These results, corresponding to the previous work [24,44], demonstrate that the magnetization value decreases with the increasing proportion of silica in the magnetic silica composite. Moreover, the magnetization curves confirm a typical feature of superparamagnetism as no hysteresis is observed in low fields. As a result, the microspheres with superparamagnetic characteristic and high magnetization value can quickly respond to the external magnetic field and quickly redisperse once the external magnetic field is removed, which is important to their applications in magnetic separation (Fig. S3, inset, SI).

3.2. Investigation of the enrichment efficiency

The efficiency of Fe_3O_4@mSiO_2-3 in peptides enrichment was studied by using Angiotensin II (MW = 1046.2, pI = 6.74, DRVYIHPF) as a model peptide followed by MALDI-TOF MS analysis. Fe_3O_4@nSiO_2 spheres were also studied for comparison. Angiotensin II at the concentration of 5 nM was detected by MS with S/N ratio of only 17.40 (Fig. 4a). After enriched by Fe_3O_4@nSiO_2 and Fe_3O_4@mSiO_2-3 spheres, the S/N ratio increased to 43.21 and 1080.14 (Fig. 4b and c), respectively. These results indicate that the enrichment efficiency of Fe_3O_4@mSiO_2-3 spheres is much better than that of Fe_3O_4@nSiO_2, due to its larger surface area and pore volume.

3.3. Study of the size-exclusion effect of Fe_3O_4@mSiO_2-3 microspheres

A unique character of the Fe_3O_4@mSiO_2-3 microspheres is their highly ordered mesopores. To investigate the size-exclusion effect of the pore structure of Fe_3O_4@mSiO_2-3 microspheres, BSA digest and several protein solutions were enriched prior to MS analysis. As shown in Fig. 4b, 10 nM BSA digest solution were hardly detected without any treatment. In the procedure of enrichment, the siloxane bridge of Fe_3O_4@mSiO_2-3 is a hydrophobic group, and therefore

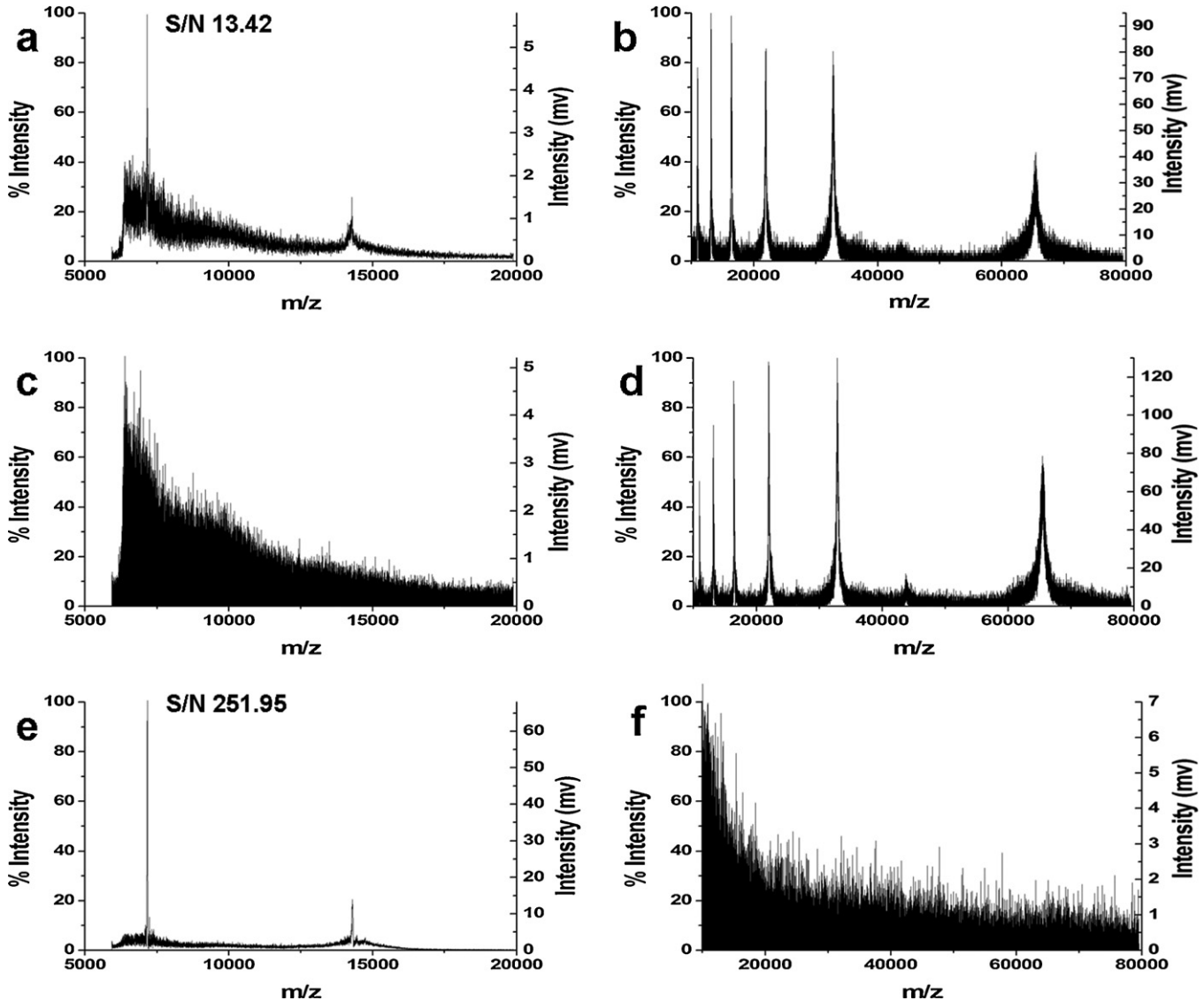

Fig. 5. MALDI-TOF mass spectra of 500 nM lysozyme solution without any treatment (a), supernate (c) and eluate (e) after enrichment with Fe_3O_4@mSiO_2-3 microspheres, mass spectra of 500 nM BSA solution without any treatment (b), supernate (d) and eluate (f) after enrichment with Fe_3O_4@mSiO_2-3 particles.

most of the peptides can be absorbed by hydrophobic interaction [13,25]. After enriched by Fe_3O_4@mSiO_2-3, no assignable signal could be observed in the supernatant (Fig. 4d), while the signals in the eluate were abundant and obvious (Fig. 4f), indicating that most of the peptides in BSA digestion were efficiently trapped by the Fe_3O_4@mSiO_2-3 microspheres. As is shown in Table S1, only 5 peptides could be detected without any treatment, while 23 peptides were detected after enrichment with Fe_3O_4@mSiO_2-3. The size-exclusion effect was further investigated with standard proteins of lysozyme (MW 14,388 Da), myoglobin (MW 17,000 Da), HRP (MW 44,000 Da) and BSA (MW 66,400 Da). The mass spectra of 500 nM lysozyme or 500 nM myoglobin in the supernatant showed no assignable signal (Fig. 5b; Fig. S4b, SI), while the S/N ratios of protein signals in the eluate solutions increased obviously (Fig. 5e; Fig. S4c, SI) compared with that without any treatment (Fig. 5a; Fig. S4a, SI). These results indicated that peptides and low-MW proteins can be enriched by Fe_3O_4@mSiO_2-3. On the contrary, the mass spectra of 500 nM HRP and 500 nM BSA in the supernatant (Fig. 5d; Fig. S5b, SI) were similar to those without any treatment (Fig. 5b; Fig. S5a, SI), while the spectra of the eluate solution displayed no assignable signal (Fig. 5f; Fig. S5c, SI). Therefore, it can be concluded that the Fe_3O_4@mSiO_2-3 microspheres can effectively exclude high-MW proteins.

3.4. Study of the desalting efficiency

During the procedures of extraction and proteolysis of proteins, some salts are normally introduced to promote the dissolution of protein and peptides. However the presence of salts can seriously interfere with MS signals [45–47]. Therefore, a desalting step is necessary prior to MS analysis. To investigate the influence of salts on the enrichment of peptides with Fe_3O_4@mSiO_2-3, 10 nM BSA digest containing 1 M NaCl or 1 M urea was enriched. According to Fig. 6a and b, no peptide signal could be observed in the presence of high-concentration salts. It is obvious that there were 20 (21) peptides enriched on the Fe_3O_4@mSiO_2-3 spheres, and the MS signals showed high S/N ratio (Fig. 6e and f). As a comparison, only 8 (7) peptides signals with low S/N ratio were observed after treated by a commercial Zip-Tip C18 pipette tip (Fig. 6c and d). These results indicated that Zip-Tip C18 had a relatively low efficiency for enriching and desalting low-abundant samples compared with Fe_3O_4@mSiO_2-3, because of the low loading capacity. Hence,

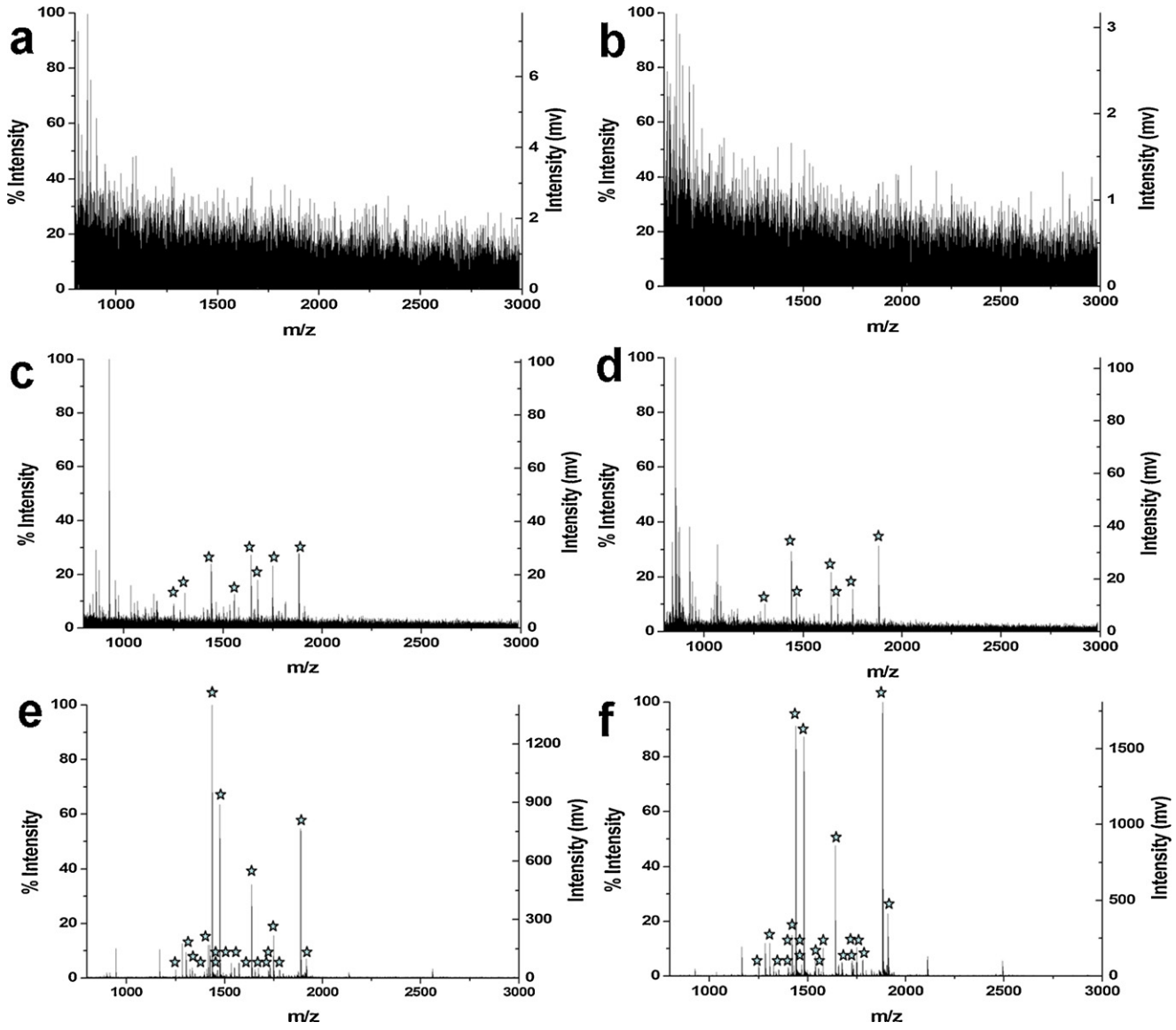

Fig. 6. MALDI-TOF mass spectra of 10 nM BSA digest with 1 M NaCl without any treatment (a), treated by a Zip-Tip C18 pipette tip (c) and enriched by Fe_3O_4@mSiO_2-3 microspheres (e), mass spectra of 10 nM BSA digest with 1 M urea without any treatment (b), treated by a Zip-Tip C18 pipette tip (d) and enriched by Fe_3O_4@mSiO_2-3 microspheres (f). Asterisks mark the peaks of the observed BSA fragments.

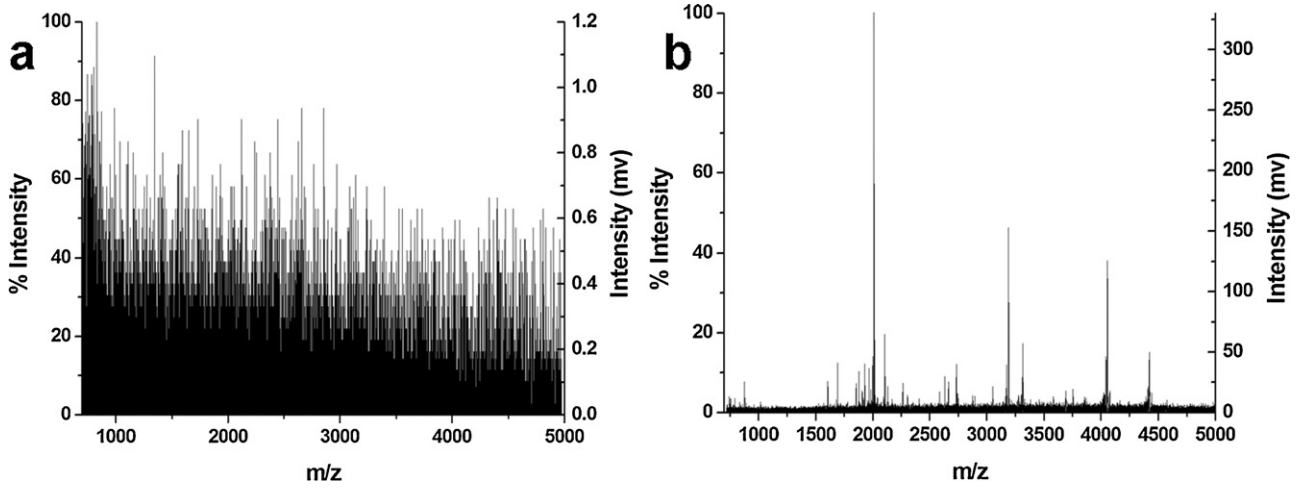

Fig. 7. MALDI-TOF mass spectra of human plasma without any treatment (a) and enriched by Fe_3O_4@mSiO_2-3 particles (b).

concentration and desalting of low-abundant sample solution with large volume and high-concentration salts can be achieved simultaneously using Fe_3O_4@mSiO_2-3.

3.5. Application in real sample

During the last decade, great efforts were made to investigate the proteome of human blood plasma. Analysis of proteins and peptides circulating in the liquid components of blood enables unique opportunities to measure the physiological and pathophysiological states of the human body [48–50]. To further confirm their superior efficiency for peptide enrichment, Fe_3O_4@mSiO_2-3 microspheres were used to extract endogenous peptides from human plasma. Directly identification of peptides in human plasma by MALDI-TOF MS analysis was difficult (Fig. 7a), because of the high-concentration salts and proteins. However, after enriched with Fe_3O_4@mSiO_2-3, many peptides were clearly observed in the spectrum (Fig. 7b). As shown in Section 2.10, the sample of human plasma was directly diluted for peptides enrichment without any other process to remove high-concentration proteins or salts, because the high-MW molecules were excluded with the material and the salts or other hydrophilic contaminants can be eliminated in the washing step. The process of the enrichment indicates that this method is facile, rapid and effective. Thus, the Fe_3O_4@mSiO_2-3 spheres have potential in concentration and separation of peptides from complex biological samples.

4. Conclusions

In summary, via pseudomorphic synthesis, Fe_3O_4@nSiO_2 microspheres were successfully transformed into Fe_3O_4@mSiO_2 particles, which possess good monodispersion, high magnetization, superparamagnetism, uniform accessible mesopores, and large surface area and pore volume. The S/N ratio of MALDI mass spectrum of Angiotensin II can be increased 62-fold after enriched by Fe_3O_4@mSiO_2. Moreover, Fe_3O_4@mSiO_2 can effectively exclude salts and high-MW proteins, and selectively enrich peptides. Furthermore, Fe_3O_4@mSiO_2 demonstrated potential applications on the rapid and effective enrichment of peptides from complex biological sample.

Acknowledgements

This work was partly supported by grants from the National Natural Science Fundation of China (91017013, 31070327), the Science Fund for Creative Research Groups (No. 20921062), NSFC, and the Fundamental Research Funds for the Central Universities. We also thank Shimadzu (China) Co. Ltd. for providing Axima TOF^2 mass spectrometry.

Appendix A. Supplementary data

Supplementary data associated with this article can be found, in the online version, at doi:10.1016/j.chroma.2011.12.045.

References

[1] E.P. Diamandis, J. Proteome Res. 5 (2006) 2079.
[2] M. Soloviev, P. Finch, Proteomics 6 (2006) 744.
[3] R.J. Tian, L.B. Ren, H.J. Ma, X. Li, L.H. Hu, M.L. Ye, R.A. Wu, Z.J. Tian, Z. Liu, H.F. Zou, J. Chromatogr. A 1216 (2009) 1270.
[4] K. Novak, Nat. Rev. Cancer 6 (2006) 92.
[5] J.Y. Ying, C.P. Mehnert, M.S. Wong, Angew. Chem. Int. Ed. 38 (1999) 56.
[6] M. Vallet-Regí, F. Balas, D. Arcos, Angew. Chem. Int. Ed. 46 (2007) 7548.
[7] L.F. Giraldo, B.L. Lopez, L. Perez, S. Urrego, L. Sierra, M. Mesa, Macromol. Symp. 258 (2007) 129.
[8] Z.X. Wu, D.Y. Zhao, Chem. Commun. 47 (2011) 3332.
[9] A. Popat, S.B. Hartono, F. Stahr, J. Liu, S.Z. Qiao, G.Q. Lu, Nanoscale 3 (2011) 2801.
[10] M.E. Davis, Nature 417 (2002) 813.
[11] M. Hartmann, Chem. Mater. 17 (2005) 4577.
[12] A. Katiyar, N.G. Pinto, Small 5 (2006) 644.
[13] R.J. Tian, H. Zhang, M.L. Ye, X.G. Jiang, L.H. Hu, X. Li, X.H. Bao, H.F. Zou, Angew. Chem. Int. Ed. 46 (2007) 962.
[14] Y.M. Huh, Y.W. Jun, H.T. Song, S. Kim, J.S. Choi, J.H. Lee, S. Yoon, K.S. Kim, J.S. Shin, J.S. Suh, J. Cheon, J. Am. Chem. Soc. 127 (2005) 12387.
[15] X.S. Li, J.H. Wu, Y. Zhao, W.P. Zhang, Q. Gao, L. Guo, B.F. Yuan, Y.Q. Feng, J. Chromatogr. A 1218 (2011) 3845.
[16] J. Won, M. Kim, Y.W. Yi, Y.H. Kim, N. Jung, T.K. Kim, Science 309 (2005) 121.
[17] R. Hao, R.J. Xing, Z.C. Xu, Y.L. Hou, S. Gao, S.H. Sun, Adv. Mater. 22 (2010) 2729.
[18] F. Caruso, M. Spasova, A. Susha, G. Michael, A.C. Rachel, Chem. Mater. 13 (2001) 109.
[19] S.I. Israel, A.R. Jose, M.M. Jose, V. Marisol, B. Enrique, J. Chromatogr. A 1218 (2011) 2196.
[20] H.M. Chen, C.H. Deng, X.M. Zhang, Angew. Chem. 122 (2010) 617.
[21] Q. Gao, D. Luo, J. Ding, Y.Q. Feng, J. Chromatogr. A 1217 (2010) 5602.
[22] J.H. Wu, X.S. Li, Y. Zhao, Q. Gao, L. Guo, Y.Q. Feng, Chem. Commun. 46 (2010) 9031.
[23] P. Wu, J. Zhu, Z. Xu, Adv. Funct. Mater. 14 (2004) 345.
[24] L. Zhang, S.Z. Qiao, Y.G. Jin, Z.G. Chen, H.C. Gu, G.Q. Lu, Adv. Mater. 20 (2008) 805.
[25] H.M. Chen, S.S. Liu, H.L. Yang, Y. Mao, C.H. Deng, X.M. Zhang, P.Y. Yang, Proteomics 10 (2010) 930.
[26] L.L. Sun, Q. Zhao, G.J. Zhu, Y. Zhou, T.T. Wang, Y.C. Shan, K.G. Yang, Zhen Liang, L.H. Zhang, Y.K. Zhang, Rapid Commun. Mass Spectrom. 25 (2011) 1257.
[27] S.S. Liu, Y. Li, C.H. Deng, Y. Mao, X.M. Zhang, P.Y. Yang, Proteomics 11 (2011) 4503.
[28] S.S. Liu, H.M. Chen, X.H. Lu, C.H. Deng, X.M. Zhang, P.Y. Yang, Angew. Chem. Int. Ed. 49 (2010) 7557.
[29] S.S. Huang, Y. Fan, Z.Y. Cheng, D.Y. Kong, P.P. Yang, Z.W. Quan, C.M. Zhang, J. Lin, J. Phys. Chem. C 113 (2009) 1775.
[30] C.Y. Lai, B.G. Trewyn, D.M. Jeftinija, K. Jeftinija, S. Xu, S. Jeftinija, V.S.Y. Lin, J. Am. Chem. Soc. 125 (2003) 4451.
[31] L. Zhang, S.Z. Qiao, Y.G. Jin, H.G. Yang, S. Budihartono, F. Stahr, Z.F. Yan, X.L. Wang, Z.P. Hao, G.Q. Lu, Adv. Funct. Mater. 18 (2008) 3203.
[32] W.R. Zhao, J.L. Gu, L.X. Zhang, H.R. Chen, J.L. Shi, J. Am. Chem. Soc. 127 (2005) 8916.
[33] X.L. Zhang, H.Y. Niu, W.H. Li, Y.L. Shi, Y.Q. Cai, Chem. Commun. 47 (2011) 4454.
[34] J. Kim, H.S. Kim, N. Lee, T. Kim, H. Kim, T. Yu, I.C. Song, W.K. Moon, T. Hyeon, Angew. Chem. Int. Ed. 47 (2008) 8438.
[35] Y.H. Deng, D.W. Qi, C.H. Deng, X.M. Zhang, D.Y. Zhao, J. Am. Chem. Soc. 130 (2008) 28.
[36] X.H. Zhang, L. Jiang, J. Mater. Chem. 21 (2011) 10653.
[37] A. Galarneau, J. Iapichella, K. Bonhomme, F.D. Renzo, P. Kooyman, O. Terasaki, F. Fajula, Adv. Funct. Mater. 16 (2006) 1657.
[38] T. Martin, A. Galarneau, F.D. Renzo, F. Fajula, D. Plee, Angew. Chem. Int. Ed. 41 (2002) 2590.
[39] B. Lefèvre, A. Galarneau, J. Iapichella, C. Petitto, F. Di Renzo, F. Fajula, Chem. Mater. 17 (2005) 601.
[40] H. Deng, Xiaolin Li, Q. Peng, X. Wang, J.P. Chen, Y.D. Li, Angew. Chem. Int. Ed. 44 (2005) 2782.
[41] W. Stöber, A. Fink, J. Colloid Interface Sci. 26 (1968) 62.
[42] Y.B. Luo, Z.G. Shi, Q. Gao, Y.Q. Feng, J. Chromatogr. A 1218 (2011) 1353.
[43] C.T. Duncan, S. Flitsch, T. Asefa, ChemCatChem 1 (2009) 365.
[44] X.Q. Chen, K.F. Lam, Q.J. Zhang, B.C. Pan, M. Arruebo, K.L. Yeung, J. Phys. Chem. C 113 (2009) 9804.
[45] H.M. Chen, D.W. Qi, C.H. Deng, P.Y. Yang, X.M. Zhang, Proteomics 9 (2009) 380.
[46] W.W. Shen, H.M. Xiong, Y. Xu, S.J. Cai, H.J. Lu, P.Y. Yang, Anal. Chem. 80 (2008) 6758.
[47] W.T. Jia, X.H. Chen, H.J. Lu, P.Y. Yang, Angew. Chem. Int. Ed. 45 (2006) 3345.
[48] X.Y. Zheng, S.L. Wu, M. Hincapie, W.S. Hancock, J. Chromatogr. A 1216 (2009) 3538.
[49] J.M. Jacobs, J.N. Adkins, W.J. Qian, T. Liu, Y.F. Shen, D.G. Camp II, R.D. Smith, J. Proteome Res. 4 (2005) 1073.
[50] H. Bernhard, S. Bettina, A. Arno, H.L. Angelika, H.L. Herbert, Electrophoresis 32 (2011) 1706.